ACS Macro Letters

Letter

pubs.acs.org/macroletters

Persistence Length of Dendritic Molecular Brushes

O. V. Borisov,*[,†,‡] E. B. Zhulina,[‡] and T. M. Birshtein[‡,§]

[†]IPREM UMR 5254 CNRS UPPA, 64053 Pau, France

[‡]Institute of Macromolecular Compounds, Russian Academy of Sciences, 199004 Saint-Petersburg, Russia

[§]Department of Physics, Saint-Petersburg State University, 198504 Petrodvorets, Saint-Petersburg, Russia

ABSTRACT: On the basis of mean-field theory, we predict that molecular brushes with dendritic side chains ("dendronized polymers") may exhibit the behavior of semirigid polymers capable of lyotropic odering. The apparent persistence length of these molecular brushes is governed by the interactions between dendritic grafts and may significantly exceed the characteristic brush thickness. Compared to bottle-brushes with linear grafts, manifestation of the induced rigidity in molecular brushes with dendritic branches is expected at smaller degrees of polymerization of the grafts. Under good solvent conditions, the induced rigidity depends solely on the number of side chain monomers per unit length of backbone and the second virial coeffcient of monomer−monomer interactions, irrespective of graft topology.

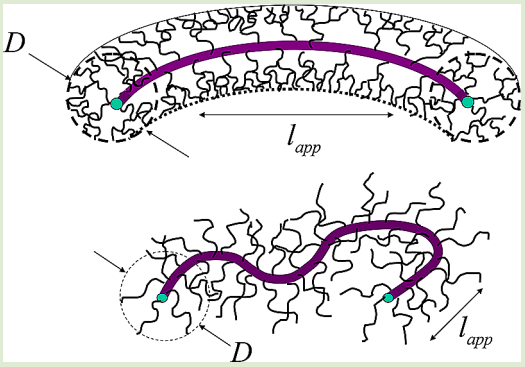

Molecular brushes consisting of a linear main chain (backbone) decorated with numerous side chains (grafts) were very much in the focus of theoretical and experimental research in the past decade.[1−4] The grafts could have different architectures including linear, comb-like, regularly or randomly branched chains, and so on (see Figure 1). The molecular brushes are characterized by high grafting density of the grafts so that neighboring side chains are considerably overlapped. Both local and large-scale conformational properties of the molecular brushes are strongly affected by repulsive (under good or theta solvent conditions) interactions between the side chains.[5,6] These repulsions lead to stretching of the grafts in the radial direction and induce strong axial tension in the main chain.[5,7]

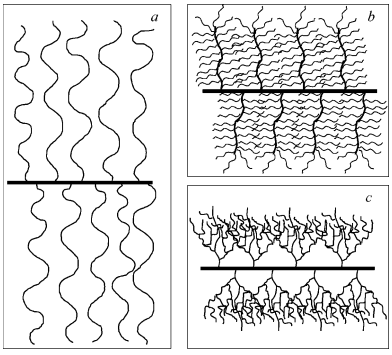

Figure 1. Schematic of molecular brushes with linear (a), comb-branched (b), and dendritically branched (c) grafts.

On the mesoscopic length scales the molecular brush can be assimilated to a wormlike chain, which is characterized by the cross-sectional thickness D (determined by radial extension of the grafts), and the apparent persistence length l_{app}. The latter arises due to extra crowding of the side chains upon bending of the molecular brush and controls bending fluctuations on the length scale comparable or larger than D. The coarse-grained "wormlike" chain model for a molecular brush with linear side chains was introduced more than two decades ago.[5] According to this model, a molecular brush in both good and theta solvents is subdivided into N_D effective (impermeable) monomers with size D and adopts the conformation of a swollen coil with average size $\sim D(l_{app}/D)^{1/5}N_D^{3/5}$. However, the dependence of apparent persistence length l_{app} on the brush parameters (degree of polymerization and grafting density of the side chains) remained an issue of discussions in the literature for a long time. According to the scaling model developed by Fredrickson,[8] l_{app} increases with increasing length of the side chains stronger than the effective thickness D of the molecular brush, $l_{app}/D \gg 1$. Therefore, on the mesoscopic length scale, molecular brushes should demonstrate the behavior of semirigid polymers capable, for example, of lyotropic ordering. On the contrary, in ref 5 it was suggested that because of repartitioning of the grafts from the concave to the convex side in bent molecular brush, the increase in the free energy upon bending is negligible, and therefore, the brush exhibits a flexible chain behavior on length scales larger than D, that is $l_{app}/D \simeq 1$. Systematic computer simulations[9−13] have indicated that the apparent persistence length l_{app} of molecular brushes increases proportionally to the brush thickness D upon an increase in the length of the grafts. The same trend follows

Received: July 31, 2012
Accepted: September 12, 2012
Published: September 18, 2012

   dx.doi.org/10.1021/mz3003903 | *ACS Macro Lett.* 2012, 1, 1166−1169

from the scattering experiments[16−21] performed on organo- and water-soluble molecular brushes with linear nonionic grafts.

The contradiction was resolved on the basis of extensive self-consistent field calculations[25] of the molecular brushes with side chain length varied over three decades. It was demonstrated that the average cross-sectional thickness (D) and the induced thermodynamic rigidity (l_{app}) follow different power law dependences on molecular weight of the grafts. Hence, in the limit of long grafts the induced rigidity should lead to large aspect ratio $l_{app}/D \gg 1$, in accordance with the prediction in ref 8. However, due to repartitioning of the grafts upon bending, the numerical factor in the expression for induced rigidity is much smaller than unity. As a result, the induced persistence length remains smaller than the cross-sectional thickness D of the brush for relatively short side chains with $\sim 10^1-10^2$ statistical segments. In this case the apparent rigidity of the brush is controlled by its cross-sectional thickness D. All experimental systems studied so far and earlier computer simulations correspond to this range of the graft lengths, that explains found proportionality $l_{app} \sim D$. Only for molecular brushes with extremely long linear grafts one could expect manifestation of the induced rigidity, and large-scale behavior of the molecular brushes as semirigid chains with aspect ratio $l_{app}/D \gg 1$. The same conclusions have been drawn on the basis of recent large-scale MC simulations.[14]

A different scenario is expected for molecular brushes with branched grafts. Below we apply the mean-field approach to examine the effect of hierarchical branching of the side chains (grafts) on the equilibrium conformations and thermodynamic stiffness of molecular brushes. We consider molecular brushes with dendritic side chains (called also "dendronized polymers")[15] and compare their properties to molecular brushes with linear grafts. As we demonstrate below, the ratio of the induced rigidity to the cross-sectional brush thickness l_{app}/D increases as a function of the degree of branching of the grafts, making feasible large-scale behavior of the molecular brushes as semirigid mesoscopic chains.

RESULTS AND DISCUSSION

We consider a molecular brush comprising of the main chain (backbone) onto which dendritically branched side chains (grafts), each of degree of polymerization N, are attached at regular intervals, see Figure 1c. A small separation h between neighboring grafting points along the backbone ensures strong lateral crowding of the grafts. We assume that the number of grafts is sufficiently large to neglect the edge effects due to finite length of the main chain.

Each of the grafts is a dendron characterized by the number of generations, $g = 0, 1, 2, ...$ The number of monomer units in a single spacer is n, and functionality of each branching point is $q \geq 1$ ($q = 1$ corresponds to linear grafts). The number of monomer units in a dendron of generation $g \geq 0$ equals $N = n(q^{g+1} - 1)/(q - 1)$. One can also introduce the number of monomer units in the longest elastic path in a dendron, from the focal point attached to the main chain to any of the terminal points. This path includes one spacer from each generation and comprises $\mathcal{N} = n(g + 1)$ monomer units. The ratio $N/\mathcal{N} = (q^{g+1} - 1)/[(q - 1)(g + 1)]$ does not depend on n and grows with an increase in both q and g. This ratio can be considered as a measure of the degree of branching in the dendrons. Obviously, for the linear chain ($g = 0$ or $q = 1$) $\mathcal{N} = N$.

We assume that spacers separating the branching points in the grafts are moderately flexible. That is, ratio of the statistical segment length, A, and the monomer length, a, in the spacer is $p = A/a > 1$. For such polymers, moderately good solvent conditions ensure the applicability of mean-field approximation to account for monomer−monomer interactions in semidilute solutions.[26,27] At relatively low monomer concentrations c, the interaction free energy per unit volume, $k_BT(va^3c^2 + wa^6c^3)$, is dominated by binary and ternary repulsions between monomers, where va^3 and wa^6 are the second and the third virial coefficients, respectively. Below we use a as the unit length. We also assume that (i) either persistence length of an isolated backbone is larger than axial distance h between neighboring grafts, or (ii) overlap of the grafts causes strong elongation of the main chain segment comprising of n_b monomers between neighboring grafting points up to $h \approx n_b$. In both scenarios, the axial distance h is independent of molecular weight N of side chains. The solution of molecular brushes is assumed to be dilute so that intermolecular interactions could be neglected.

The free energy of molecular brush (per graft) can be represented as

$$F(D) = F_{int}(D) + F_{conf}(D) \tag{1}$$

In terms of averaged polymer density within thickness D, the contribution due to excluded volume repulsions between the grafts is formulated as

$$\frac{F_{int}(D)}{k_BT} \cong \begin{cases} vN^2D^{-2}h^{-1}, & \text{good solvent} \\ wN^3D^{-4}h^{-2}, & \text{theta solvent} \end{cases} \tag{2}$$

regardless of the graft topology.

On the contrary, the conformational free energy that accounts for entropy losses in the extended grafts, should be specified for a particular graft topology. In the dendritic graft one can define multiple elastic paths of length $\mathcal{N}$ connecting the focal (grafting) point to any of the terminal groups. Consequently, one can identify two limits for the conformational entropy losses in extended dendrons,[23]

$$\frac{F_{conf}(D)}{k_BT} \cong \frac{D^2}{p\mathcal{N}}\left(\frac{N}{\mathcal{N}}\right)^{\beta-1} \qquad \beta = 1, 2 \tag{3}$$

The minimal conformational entropy penalty ($\beta = 1$) occurs upon stretching of an (arbitrary) longest elastic part within each dendron, whereas the spacers not belonging to this path remain unstretched. In the opposite limiting scenario ($\beta = 2$), all the spacers in all the generations are uniformly stretched that leads to maximal estimate for the conformational entropy losses at given size of the dendrons.

Minimization of the free energy F with respect to D gives

$$D \cong \begin{cases} (vph^2)^{1/4}(N/h)^{3/4}(\mathcal{N}/N)^{\beta/4}, & \text{good solvent} \\ (wph^2)^{1/6}(N/h)^{2/3}(\mathcal{N}/N)^{\beta/6}, & \text{theta solvent} \end{cases} \tag{4}$$

As is seen from eq 4, at fixed values of N and h, the cross-sectional thickness D decreases upon an increase in degree of branching $N/\mathcal{N}$. By substituting D (eq 4) in eqs 1−3, we find the equilibrium free energy per graft

$$\frac{F(D)}{k_BT} \cong \begin{cases} (v/ph)^{1/2}N^{1/2}(N/\mathcal{N})^{\beta/2}, & \text{good solvent} \\ (w/p^2h^2)^{1/3}N^{1/3}(N/\mathcal{N})^{2\beta/3}, & \text{theta solvent} \end{cases} \tag{5}$$

dx.doi.org/10.1021/mz3003903 | ACS Macro Lett. 2012, 1, 1166−1169

The induced persistence length l_{app} of molecular brush is specified as[25]

$$l_{app} \cong \frac{D^2 F(D)}{hk_B T} \tag{6}$$

Here, D and $F(D)$ are the equilibrium brush thickness and the free energy per graft, respectively, in an unperturbed (straight) configuration. By substituting D (eq 4) and $F(D)$ (eq 5) in eq 6, one finds the power law dependences for induced persistence length

$$l_{app} \cong \begin{cases} \nu(N/h)^2, & \text{good solvent} \\ (w^2/ph^2)^{1/3}(N/h)^{5/3}(N/\mathcal{N})^{\beta/3}, & \text{theta solvent} \end{cases} \tag{7}$$

Remarkably, under good solvent conditions, l_{app} is independent of the thermodynamic rigidity of the grafts $p > 1$, degree of branching $N/\mathcal{N}$, and "mode" of the elastic stretching. Such a behavior of l_{app} follows directly from eqs 1, 2, and 6. Because at equilibrium both contributions in eq 1 are on the same order of magnitude ($F_{int}(D) \simeq F_{conf}(D)$), under good solvent conditions, the free energy per graft $F(D) \simeq F_{int}(D) \sim D^{-2}$, and therefore, $l_{app} \sim F(D)D^2 \sim D^0$ (eq 6) depends only on the graft molecular mass per unit length of the backbone, N/h, and the second virial coefficient ν.

An increase in branching parameter $N/\mathcal{N}$ leads, however, to an increase in average monomer concentration $c \simeq N/hD^2$ and to the corresponding transition (at $c > \nu/w$) from the good- to theta-solvent regime for side chains. The boundary $\nu = \nu^* \simeq wc$ between good- and theta-solvent regimes is specified as

$$\nu^* \simeq \left(\frac{w^2}{phN}\right)^{1/3}\left(\frac{N}{\mathcal{N}}\right)^{\beta/3} \tag{8}$$

Under theta-solvent conditions ($\nu < \nu^*$), l_{app} is determined by the second line in eq 7. As follows from eqs 4 and 7, both D and l_{app} are increasing functions of the grafting density, $1/h$. However, at given value of N, the brush thickness D decreases as a function of the degree of branching, $N/\mathcal{N}$. At $N/\mathcal{N} \cong 1$, the scaling expressions for the brush thickness and induced rigidity are equivalent to those for molecular brush with linear grafts.[5,25]

Manifestation of the induced rigidity in the large-scale conformational properties of the molecular brush depends crucially on the ratio of the induced rigidity to the cross-sectional brush thickness D:

$$\frac{l_{app}}{D} \cong \begin{cases} (\nu^3/ph^2)^{1/4}(N/h)^{5/4}(N/\mathcal{N})^{\beta/4}, & \text{good solvent} \\ (w/ph^2)^{1/2}(N/h)(N/\mathcal{N})^{\beta/2}, & \text{theta solvent} \end{cases} \tag{9}$$

When $l_{app}/D \gg 1$, the induced rigidity causes stiffening of the brush on length scales larger than D and the brush behaves as a semiflexible wormlike chain of effective monomers with size D. In the opposite limit, the flexibility of molecular brush on length scales $\geq D$ is controlled by its thickness D, and the brush behaves as a flexible chain of effective monomers with $l_{app} \simeq D$. In scaling terms, inequality $l_{app} > D$ is always fulfilled when the side chains are found in the brush regime. However, the numerical coefficient omitted in eq 7 could be much less than unity, and numerically, the condition $l_{app} > D$ might be satisfied only starting from certain molecular weight of the grafts.

In Figure 2 we present the asymptotic dependences of induced persistence length l_{app} and apparent aspect ratio l_{app}/D

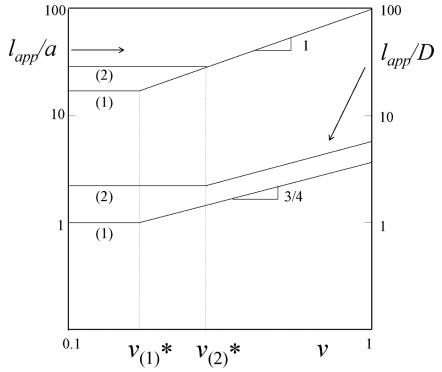

Figure 2. Asymptotic power law dependences of induced persistence length l_{app}/a (eq 7) and of aspect ratio l_{app}/D (eq 9) as a function of dimensionless (normalized by a^3) second virial coefficient ν of monomer−monomer interactions for linear grafts, $N/\mathcal{N} = 1$ (1) and for strongly branched grafts $N/\mathcal{N} = 4.33$ (2) (which corrresponds to dendrons with $g = 2$, $q = 3$). Values of other parameters are: number of monomers in the graft $N = 100$, distance between the grafts $h = 2a$, $p = A/a = 1$, dimensionless (normalized by a^6) third virial coefficient $w = 1$. The numerical coefficient in eq 4 is set to unity, the numerical coefficient in eq 9 is set to 0.04 in order to provide $l_{app}/D \approx 1$ for linear grafts in accordance to SCF calculations in ref 25. The slopes are indicated near the curves.

as a function of solvent strength ν for weakly branched (with $(N/\mathcal{N}) \simeq 1$) and strongly branched (with $(N/\mathcal{N})_2 \gg (N/\mathcal{N})_1$) side chains. In both cases, l_{app} and l_{app}/D are increasing functions of ν in good solvent regime $\nu \geq \nu^*$. However, the theta-region, where the brush properties are independent of solvent strength, expands with increasing degree of branching. As it follows from eqs 9 and Figure 2, aspect ratio l_{app}/D increases as a function of N and, for given N, as a function of the degree of branching $N/\mathcal{N}$. In molecular brushes with strongly branched dendritic grafts with $N/\mathcal{N} \gg 1$, the crossover from flexible to semirigid wormlike chain behavior might therefore occur at a smaller degree of polymerization N of the grafts.

Experiments have demonstrated that polymers with dendritically branched side groups exhibit enhanced thermodynamic stiffness, which is manifested in increased persistence length.[28,29] However, systematic comparison between molecular brushes with linear and dendritic grafts is currently lacking.

To the end, we briefly discuss the conformations and induced rigidity of the molecular brushes with comb-like grafts, see Figure 1b. The latter could mimic certain natural biomacromolecular assemblies, for example, aggrecan in articular cartilage.[30] The aggrecan assembly comprises a very long hyaluronan backbone with grafted aggrecan "monomers"—comb-like brushes consisting of protein main chain and polysaccharide side chains. Polysaccharides in aggrecan monomers are semiflexible ($p > 1$) and are strongly ionized with fraction of charged monomers $\alpha \lesssim 1$. Under relatively high salt concentrations (close, e.g., to physiological conditions), the electrostatic interactions between monomers in ionized (polyelectrolyte) brushes manifest themselves via an effective second virial coefficient $\nu_{eff} \simeq \alpha^2/c_s$, where c_s is the concentration of salt ions. Therefore, one can apply the results for good solvent conditions (with modified second virial

dx.doi.org/10.1021/mz3003903 | ACS Macro Lett. 2012, 1, 1166−1169

coefficient $v \rightarrow v + v_{eff}$) to describe the aggrecan brush. In the first approximation, each of the comb-shaped grafts (aggrecan monomers) could be modeled as a linear main chain of $\mathcal{N}$ monomer units with grafted to it with intervals m side chains, each of length n. Hence, $N = \mathcal{N}(1 + n/m)$ is the number of monomers in one comb-shaped graft. The ratio $n/m \approx N/\mathcal{N}$ characterizes the degree of branching of the comb-like grafts. A unique longest elastic path in each graft coincides with its main chain. Therefore, the conformational free energy of the brush with comb-like grafts is given by eq 5 with $\beta = 1$. As discussed above, the induced rigidity l_{app} of a molecular brush in a good solvent does not depend on the degree of branching (that is, n/m in case of comb-like grafts). Aging is known to affect the grafting density of side chains in aggrecan monomers.[30] According to our results, at a fixed distance h between the grafts, detachment of side chains in comb-like aggrecan monomers leads to the decrease in mass per unit length N/h and the corresponding increase in flexibility of the molecular brush (aggrecan assembly). This could, in turn, affect the mechanical properties of cartilage network.

To conclude (i) the induced persistence length l_{app} of a molecular brush increases with improving solvent quality for the side chains and is maximal under good solvent conditions; (ii) in a mean-field approximation, the induced persistence length l_{app} of a molecular brush in a good solvent is independent of graft topology, mode of its elastic stretching, and thermodynamic stiffness of the side chains, and is solely determined by the molecular mass of side chain per unit length of the backbone, N/h; (iii) an increase in the degree of graft branching $N/\mathcal{N}$ leads to the decrease in cross-sectional thickness D, and the corresponding increase in apparent aspect ratio l_{app}/D in both good and theta solvents. The latter makes feasible manifestation of the induced rigidity in semiflexible chain behavior of molecular brushes with sufficiently strongly branched grafts.

AUTHOR INFORMATION

Corresponding Author

*E-mail: oleg.borisov@univ-pau.fr.

Notes

The authors declare no competing financial interest.

ACKNOWLEDGMENTS

This work has been partially supported within Scientific and Technological Cooperation Program Switzerland-Russia, Grant Agreements No. 128308, by the Russian Foundation for Basic Research (Grant 11-03-00969a) and by Department of Chemistry and Material Science of the Russian Academy of Sciences.

REFERENCES

(1) Li, C.; Gunari, N.; Fischer, K.; Janshoff, A.; Schmidt, M. *Angew. Chem., Int. Ed.* **2004**, *43*, 1101.

(2) Zhang, M.; Müller, A. H. E. *J. Polym. Sci., Part A: Polym. Chem.* **2005**, *43*, 3461.

(3) Sheiko, S. S.; Sumerlin, B. S.; Matyjaszewski, K. *Prog. Polym. Sci.* **2008**, *33*, 759.

(4) Junk, M. J. N.; Li, W.; Schlüter, D.; Wegner, G.; Spiess, H. W.; Zhang, A.; Hinderberger, D. *Angew. Chem.* **2010**, *122*, 5818.

(5) Birshtein, T. M.; Borisov, O. V.; Zhulina, E. B.; Khokhlov, A. R.; Yurasova, T. A. *Polym. Sci. USSR* **1987**, *29*, 1293.

(6) Borisov, O. V.; Birshtein, T. M.; Zhulina, E. B. *Polym. Sci. USSR* **1987**, *29*, 1552.

(7) Panyukov, S.; Zhulina, E. B.; Sheiko, S. S.; Randall, G. C.; Brock, J.; Rubinstein, M. *J. Phys. Chem. B* **2009**, *113*, 3750.

(8) Fredrickson, G. *Macromolecules* **1993**, *26*, 2825.

(9) Rouault, Y.; Borisov, O. V. *Macromolecules* **1996**, *29*, 2605.

(10) Saariaho, M.; Ikkala, O.; Szleifer, I.; Erukhimovich, I.Ya.; ten Brinke, G. *J. Chem. Phys.* **1997**, *107*, 3267.

(11) Saariaho, M.; Szleifer, I.; Ikkala, O.; ten Brinke, G. *Macromol. Theor. Simul.* **1998**, *7*, 211.

(12) Subbotin, A.; Saariaho, M.; Ikkala, O.; ten Brinke, G. *Macromolecules* **2000**, *33*, 3447−3452.

(13) Hsu, H.-P.; Paul, W.; Binder, K. *Macromol. Theor. Simul.* **2007**, *16*, 660; *Phys. Rev. Lett.* **2009**, *103*, 198301; *Macromolecules* **2010**, *43*, 3094−3102.

(14) Hsu, H.-P.; Paul, W.; Binder, K. *Europhys. Lett.* **2010**, *92*, 28003.

(15) Schlüter, A. D. *Top. Curr. Chem.* **1998**, *197*, 165; *ibid* **2005**, *245*, 151−191.

(16) Lecommandoux, S.; Checot, F.; Borsali, R.; Schappacher, M.; Deffieux, A.; Brulet, A.; Cotton, J. P. *Macromolecules* **2002**, *35*, 8878.

(17) Zhang, B.; Gröhn, F.; Pedersen, J. S.; Fischer, K.; Schmidt, M. *Macromolecules* **2006**, *39*, 8440−8450.

(18) Feuz, L.; Strunz, P.; Geue, T.; Textor, M.; Borisov, O. V. *Eur. Phys. J. E* **2007**, *23*, 237.

(19) Bastardo, L.; Iruthayaraj, J.; Lundin, M.; Dedinaite, A.; Vareikis, A.; Makuska, R.; van der Wal, A.; Furo, I.; Garamus, V. M.; Claesson, P. M. *J. Colloid Interface Sci.* **2007**, *312*, 21.

(20) Cheng, G.; Melnichenko, Y. B.; Wignall, G. D.; Hua, F.; Hong, K.; Mays, J. W. *Macromolecules* **2008**, *41*, 9831.

(21) Bolisetty, S.; Rosenfeld, S.; Rochette, C. N.; Harnau, L.; Lindner, P.; Xu, Y.; Müller, A. H. E.; Ballauff, M. *Colloid Polym. Sci.* **2009**, *287*, 129.

(22) Kröger, M.; Peleg, O.; Halperin, A. *Macromolecules* **2010**, *43*, 6213−6224.

(23) Polotsky, A. A.; Gillich, T.; Borisov, O. V.; Leermakers, F. A. M.; Textor, M.; Birshtein, T. M. *Macromolecules* **2010**, *43*, 9555.

(24) Merlitz, H.; Wu, C.-X.; Sommer, J.-U. *Macromolecules* **2011**, *44*, 7043−7049.

(25) Feuz, L.; Leermakers, F. A. M.; Textor, M.; Borisov, O. V. *Macromolecules* **2005**, *38*, 8891−8901.

(26) Birshtein, T. M. *Polym. Sci. USSR* **1982**, *A24*, 2410.

(27) Shaefer, W.; Joanny, J.-F.; Pincus, P. *Macromolecules* **1980**, *13*, 1280−1289.

(28) Tsvetkov, N. V.; Andreeva, L. N.; Bushin, S. V.; Strelina, I. A.; Bezrukova, M. A.; Girbasova, N. V.; Bilibin, A.Yu. *Polym. Sci. (Russia)* **2010**, *C52*, 3−16.

(29) Chen, Y.; Xiong, X. *Chem. Commun.* **2010**, *46*, 5049−5060.

(30) Dudhia, J. *Cell. Mol. Life Sci.* **2005**, *62*, 2241−2256.